Available online at www.sciencedirect.com
SCIENCE DIRECT®
Journal of Catalysis 222 (2004) 227–237
JOURNAL OF CATALYSIS
www.elsevier.com/locate/jcat

Modification of acid supports by solid-state redox reaction Part I. Preparation and characterization

A. Hagen,[a,b,*] E. Schneider,[c] A. Kleinert,[c] and F. Roessner[c]

[a] *Technical University of Denmark, Department of Chemistry/Interdisciplinary Research Center for Catalysis, Building 312, DK-2800 Kongens Lyngby, Denmark*

[b] *Risoe National Laboratory, Materials Research Department, Building 228, P.O. Box 49, Frederiksborgvej 399, DK-4000 Roskilde, Denmark*

[c] *Carl v. Ossietzky University Oldenburg, Faculty of Mathematics and Natural Sciences, Institute of Pure and Applied Chemistry/Industrial Chemistry 2, D-26111 Oldenburg, Germany*

Received 28 July 2003; revised 24 October 2003; accepted 30 October 2003

Abstract

The solid-state redox reaction of a number of metals in contact with ZSM-5 and Y zeolites, γ-alumina, and silica was investigated by temperature-programmed hydrogen evolution (TPHE), diffuse reflectance Fourier transform IR spectroscopy (DRIFT), X-ray absorption near-edge structure spectroscopy (XANES), and X-ray powder diffraction (XRD). Among all studied metals, gallium, zinc, manganese, and iron were found to undergo a solid-state redox reaction. On zeolites, Brønsted acid sites and extraframework species and on γ-alumina all kinds of hydroxyl species are involved, whereas on silica silanol groups undergo reaction. Magnesium, on the other hand, reacted with the water adsorbed on the supports to magnesium oxide evolving hydrogen. No reaction was observed for the systems with nickel, aluminum, and tin. The solid-state redox reaction was found to be a function of the melting point provided that the metal is base enough.
© 2003 Elsevier Inc. All rights reserved.

Keywords: Solid-state redox reaction; Zeolite; TPHE; XRD; DRIFT; XANES

1. Introduction

Catalyst supports hosting cationic species have been studied in many reactions. Thus, gallium or zinc-exchanged ZSM-5 zeolites have been found useful for the conversion of lower alkanes into aromatic hydrocarbons [1]; other metal ions were also tested [1,2]. Iron-containing zeolites have been studied in the selective catalytic reduction of NO [3,4] or the oxidation of aromatic hydrocarbons [5], nickel ion-exchanged zeolites in the oligomerization of olefins [6], and Mg-ZSM-5 zeolites in the alkylation of toluene with methanol [7].

The conventional method for the preparation of those types of modified supports is ion exchange, mostly in aqueous solution. This method has, however, a number of drawbacks. It is, for example, difficult to achieve higher exchange degrees when multivalent cations have to be introduced. Usually, multifold exchange steps must be performed in order to increase the exchange degree. This in turn is accompanied by a large amount of chemicals and waste to be handled and, furthermore, it is time consuming. As an alternative to overcome these drawbacks, solid-state reactions have attracted attention. Usually, metal salts or oxides react with an acidic support [8–11]. Recent examples are the preparation of Mg-ZSM-5 zeolite for toluene alkylation by using $MgCl_2$ [12] and Fe-ZSM-5 zeolite for the decomposition of N_2O by using $FeSO_4$ [13].

Using oxidic precursors, the solid-state ion exchange between ZnO and H-ZSM-5,

$$\mathrm{ZnO} + 2\mathrm{H\text{-}zeolite} \rightarrow \mathrm{Zn^{2+}\text{-}(zeolite)_2} + \mathrm{H_2O}, \quad (1)$$

has been studied and proven to result in a catalyst with the same catalytic properties in the conversion of ethane as the conventionally prepared one [14]. This reaction can be regarded as the solid-state analogue to the dissolving of zinc oxide in liquid acids. Further, the solid-state reaction between metallic zinc and various zeolites,

$$\mathrm{Zn} + 2\mathrm{H\text{-}zeolite} \rightarrow \mathrm{Zn^{2+}\text{-}(zeolite)_2} + \mathrm{H_2}, \quad (2)$$

* Corresponding author.
E-mail address: anke.hagen@risoe.dk (A. Hagen).

0021-9517/$ – see front matter © 2003 Elsevier Inc. All rights reserved.
doi:10.1016/j.jcat.2003.10.015

came into focus [15–18] as an alternative reaction. Also this reaction has its counterpart in solution.

In addition to the shortening of modification time, decrease of amounts of chemicals, and easier achievement of high exchange degrees another advantage over liquid-phase methods has been found: the alteration of the population of cationic positions as reported for zinc reacting with Y zeolite [16,19].

As a result of their studies of the system zinc plus ammonium mordenite and Y zeolite, Beyer et al. [17] emphasized the possibilities of this reaction for the characterization of the number as well as strength of Brønsted acid sites in zeolites. This is possible, because zinc reacts with the entire number of Brønsted acid sites. When ZSM-5 zeolites were used instead, the obtained zinc-containing samples showed the same catalytic activity in the nonoxidative conversion of ethane as the samples prepared by conventional liquid-phase methods [18] revealing a new economic and environmentally friendly way to prepare transition metal ion-promoted zeolite catalysts.

The aim of the present paper is to study the solid-state redox reaction in more detail. A thorough characterization will provide information about the involved and formed species and their properties. Analogous to the liquid phase, the acid properties of the support should have importance for the redox reaction to proceed. Thus, catalyst supports with different types, numbers, and strengths of acid sites were used in this study: ZSM-5 and Y zeolites in their protonic as well as ammonia forms, γ-alumina, and finally silica, which entirely contains silanol groups though they are usually considered nonacidic.

When regarding the metal to be reacted, the electrochemical potential is the deciding factor in the liquid phase. Studying solid acid phases, another parameter must be considered, namely to provide the contact between metal and acid sites. Whereas protons are quite mobile in solution and easily approach the metal, they are more localized in the solid supports because of the positioning of the counterion in the framework. Although protons are still somewhat mobile there depending on the acid strengths of the corresponding sites, they are nevertheless apart from the metal particles. Consequently, the metal has to diffuse to the acid sites, which could be facilitated by melting, thereby enhancing its mobility. The melting point of the metal becomes an important parameter in this way. Accordingly a number of metals were chosen having a broad range of electrochemical potentials as well as melting points: gallium, tin, zinc, magnesium, aluminum, manganese, nickel, and iron.

2. Experimental

2.1. Catalysts

Commercial zeolite samples (H-ZSM-5, NH_4-ZSM-5, AlSiPenta; Si/Al molar ratio, 13.5; template-free synthesis; H-Y, NH_4-Y, Suedchemie; Si/Al molar ratio, 2.75), SiO_2 (Aldrich Davisil), and γ-alumina (LaRoche Industries Inc.) were used. The mixtures between metals (zinc (Riedel de Haën), gallium (Carl Roth), magnesium (Riedel de Haën), manganese (Riedel de Haën), iron (Merck), nickel (STREM Chemicals), aluminum (Merck), and tin (Fluka)) and support were prepared by grinding the two components in a ball mill for 4 h to give a metal content of usually 2 wt% (denoted as *Me + support*).

The resulting powders were usually pelleted, crushed, and sieved to a particle size of 200–315 μm.

2.2. Characterization

The experiments of temperature-programmed hydrogen evolution (TPHE) were performed in a unit for temperature-programmed studies (Raczek, Germany). The sample (0.5 g) was heated in an argon flow of 60 ml/min first to 473 K, kept there for 2 h to remove adsorbed water, and then heated to 1123 K. The heating rates were 10 K/min. Evolving gases were detected by a thermal conductivity detector and a MS gas analyzer (OmniStar GSD 300 O, Pfeiffer, Germany). The latter turned out to be indispensable to discriminate between the desorbed species and was additionally installed, improving the previously used experimental setup [18]. All samples subjected to this procedure are designated as TPHE-treated samples.

The DRIFT spectra were recorded with a Bruker Equinox 55 FTIR spectrometer using a purged Praying Mantis diffuse reflection arrangement equipped with a reaction chamber with low-pressure dome (Harrick) that allowed temperature-programmed investigations. The samples were mixed with inert material (diamond powder) and heated up to 873 K in a nitrogen flow of 60 ml/min. The spectra were measured at a resolution of 4 cm^{-1} with 1000 scans being averaged in the range between 7000 and 500 cm^{-1}. A mixture of diamond powder and potassium bromide was used as a standard (background) (personal communication, E. Loeffler, Ruhr University Bochum, Germany, 2002) and measured with 2000 scans being averaged. The diffuse reflection arrangement was flushed with dry air and a MCT detector was used. The reflectance values were converted into negative logarithmic function of reflectance ($-\log R$).

XANES spectra were taken at DESY (Hamburger Synchrotronstrahlungslabor, Germany) at station E4. The radiation was monochromatized by two independently driven Si(111) crystals. Samples were pressed into self-supporting sample wafers and placed on a vertical sample holder. Spectra were recorded from 9.59 to 9.90 keV in transmission mode. Simultaneously, Zn foil was measured as reference and used for energy correction (first inflection point, Zn *K* edge: 9.659 keV). Raw data were further corrected for background using a Victoreen fit in the preedge region and subtracting this function from the spectrum. The edge jump was normalized to one in the region after the main edge (continuum).

XRD measurements were performed on a Philips Analytical X-ray PC-APD system using copper anodes ($\alpha_1 = 1.54056$ Å, $\alpha_2 = 1.54439$ Å). The range was from 5 to 90° 2Θ with a step size of 0.02.

3. Results

3.1. TPHE

TPHE studies were carried out to observe hydrogen evolution that is connected with the solid-state redox reaction (see Eq. (2)). Selected TPHE spectra for zinc-containing mixtures based on the TCD signal are displayed in Fig. 1. The temperatures of hydrogen evolution and the measured hydrogen amounts based on the MS signal are summarized in Table 1 for all samples.

A NH_4-ZSM-5 zeolite was subjected to the TPHE treatment as reference (Fig. 1, spectrum I). A broad peak of low intensity appeared between around 540 to 780 K, arising from desorbing water and ammonia. This broad peak was also observed in case of Zn+NH_4-ZSM-5 zeolite (Fig. 1, spectrum II) and of all other mixtures of zinc with the ammonium forms of zeolites. This broad peak was topped by a sharper one around 714 K (Fig. 1, spectrum II), which represented the evolution of hydrogen as analyzed by the MS detector. The TPHE spectrum of Zn+H-ZSM-5 zeolite showed a high temperature peak at 912 K (Fig. 1, spectrum III). Using Zn+H-Y zeolite, a high temperature peak was observed as well whereas the Zn+NH_4-Y zeolite sample exhibited a broad peak in the low temperature region (Table 1). On Zn+SiO_2, a high temperature peak around 943 K was obtained (Fig. 1, spectrum IV).

Although the temperatures of maximum hydrogen evolution varied only slightly in the range between 910 and 960 K (Table 1), the following sequence for increasing values can be established:

$$\text{Zn+H-ZSM-5} < \text{Zn+H-Y} < \text{Zn+SiO}_2 < \text{Zn+}\gamma\text{-Al}_2\text{O}_3.$$

The ammonia forms of ZSM-5 and Y zeolite both had low-temperature peaks when heated with zinc and deviated thus significantly from the other supports.

The amount of zinc that reacted with the supports was studied for the mixtures Zn+H-ZSM-5 and Zn+NH_4-ZSM-5 zeolites in more detail. There are two theoretic values given in Fig. 2 along with the measured results. One was calculated for the reaction of zinc with the protons and ammonium ions present in the zeolite, respectively. This value is limited by the exchange capacity of the zeolite, i.e., when all protons/ammonium ions have been involved in the reaction. The other value is based on the reaction of all submitted zinc. This value does consequently not depend on the amount of protons in the zeolite and could increase unlimitedly.

When the zinc content was increased in the mixture with H-ZSM-5 zeolite, the temperature of the peak maximum for hydrogen evolution shifted to lower values (Fig. 2a). The amount of formed hydrogen increased up to the sample having a zinc content of 5 wt% and followed the theoretic value assuming that all protons of the H-ZSM-5 zeolite react. On the mixtures of zinc with NH_4-ZSM-5 zeolite, the peak temperature was not much influenced by the zinc content (Fig. 2b). The amount of evolved hydrogen increased with the amount of zinc submitted in the mixture. At higher zinc content (5 and 8 wt%), the amount of evolved hydrogen exceeded the theoretic value calculated according to the number of ammonium ions/protons in the zeolite significantly. In case of the 5 wt% Zn+NH_4-ZSM-5 sample, even the value for the reaction of all submitted zinc is exceeded, implying that there is an additional source for hydrogen. In addition to hydrogen, the evolution of nitrogen was observed and a second peak appeared in the TPHE spectrum at higher temperatures (around 940–960 K) on this sample.

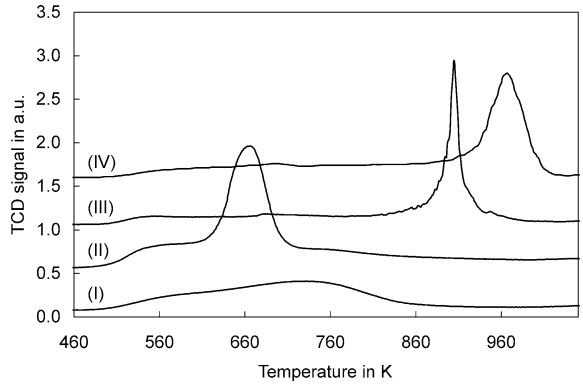

Fig. 1. TPHE spectra of NH_4-ZSM-5 (I), 2 wt% Zn+NH_4-ZSM-5 (II), 2 wt% Zn+H-ZSM-5 (III), and 4 wt% Zn+SiO_2 (IV).

Table 1
Temperatures and amounts for hydrogen evolution (based on MS signal) of Me + supports; metal content was 2 wt%

	SiO_2	H-ZSM-5	NH_4-ZSM-5	H-Y	NH_4-Y	γ-Al_2O_3
Ga (287 µmol/g)						
H_2 (µmol/g)	222	160	288	219	302	289
T (K)	698	693	699	713	693	709
Zn (306 µmol/g)						
H_2 (µmol/g)	281	328	298	241	229	307
T (K)	943	912	714	931	675	960
Mg (823 µmol/g)						
H_2 (µmol/g)	605	384	676	434	576	547
T (K)[a]	725	759	768	830	834	889
Mn (364 µmol/g)						
H_2 (µmol/g)	281	258	310	268	233	–
T (K)	952	981	977	994	993	–
Fe (358 µmol/g)						
H_2 (µmol/g)	104	111	108	106	120	180
T (K)	1076	1111	1113	1110	1064	995

The calculated amounts of hydrogen based on stoichiometric considerations are given in parentheses.

[a] The temperature given corresponds to the most intensive peak. In addition there were a number of small peaks and shoulders.

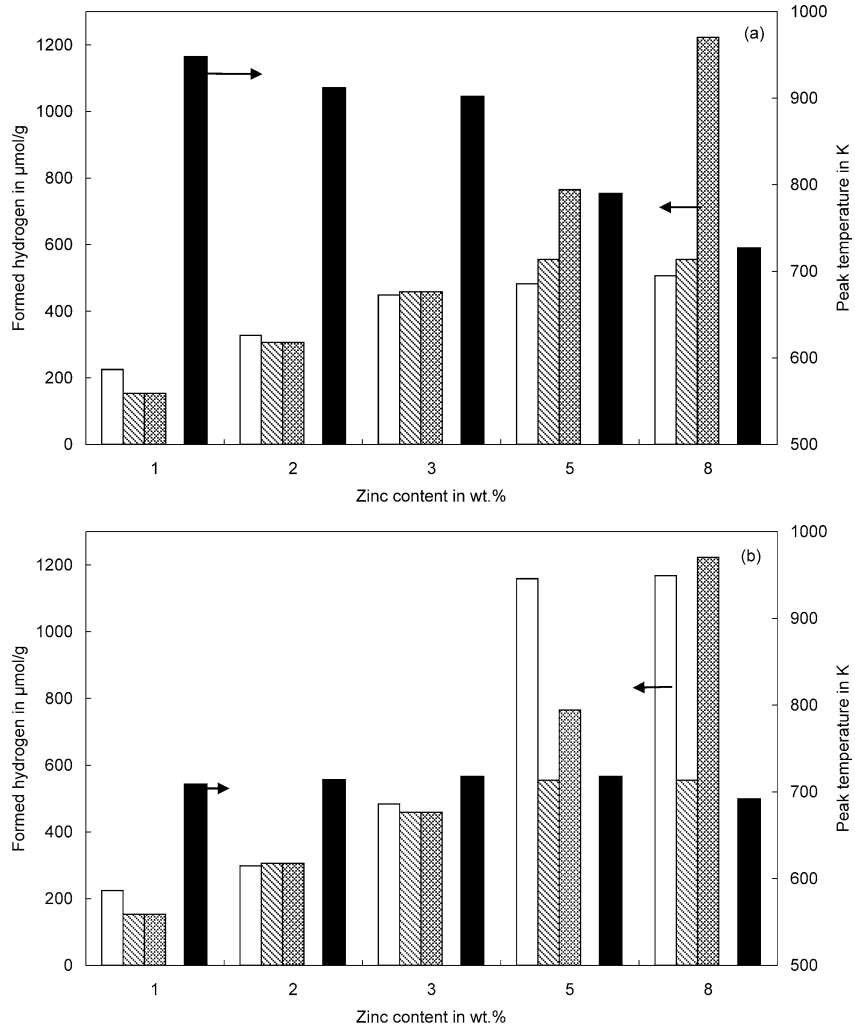

Fig. 2. Amount of hydrogen formed in the TPHE experiment (white columns), theoretic amount for reaction of zinc with protons (striped columns), and for reaction of all submitted zinc in the mixture (hatched columns). Peak temperature of hydrogen evolution (black columns, right axis) on mixtures of (a) Zn+H-ZSM-5 and (b) Zn-NH_4-ZSM-5.

On the mixture of gallium with ZSM-5 and Y zeolites, γ-alumina, and silica, hydrogen evolution peaks around 700 K were found for all supports (Table 1). This value was lower than on the mixtures of zinc with these supports (except the Zn+NH_4 zeolite samples).

Hydrogen evolution was also observed on the mixtures of magnesium with the supports in a broad temperature range (720–1110 K) with a number of peaks and shoulders appearing. The temperatures for the main peak observed on each sample are displayed in Table 1.

On the mixtures of manganese with ZSM-5 and Y zeolites and silica, hydrogen evolution temperatures were in the range of ∼950–990 K and for iron ∼995–1110 K (Table 1).

Deviating from this trend, γ-alumina did not react with manganese by redox reaction because no hydrogen formation was observed. It is also noteworthy that for the sample Fe+γ-Al_2O_3 the temperature of maximum hydrogen evolution ($T_{max} = 995$ K) was much lower than for the mixtures of iron with all other supports (Table 1). Using the other metals, namely tin, nickel, and aluminum, no traces of hydrogen were found in the TPHE experiments.

3.2. DRIFT

In the in situ DRIFT spectra, absorption bands assigned to combination vibrations and bonding vibrations of bridging hydroxyl groups (4630 and 3590 cm^{-1}, respectively) were observed at 823 K on both H- and NH_4-ZSM-5 zeolites. These bands decreased upon heating of the zeolites with Zn (Figs. 3a and 3c, spectra I and II). The intensity of the band at 3730 cm^{-1} representing silanol groups remained unaffected. In the spectrum of the Zn+H-ZSM-5 sample, a band at 3650 cm^{-1} was found which can be attributed to the AlOH vibrations of nonframework aluminum species [20]. This band decreased under heating (Figs. 3a and 3c, spectrum II).

In the faujasite structure there are crystallographically different types of oxygen and therefore different corresponding types of hydroxyl groups. Two overlapping bands at

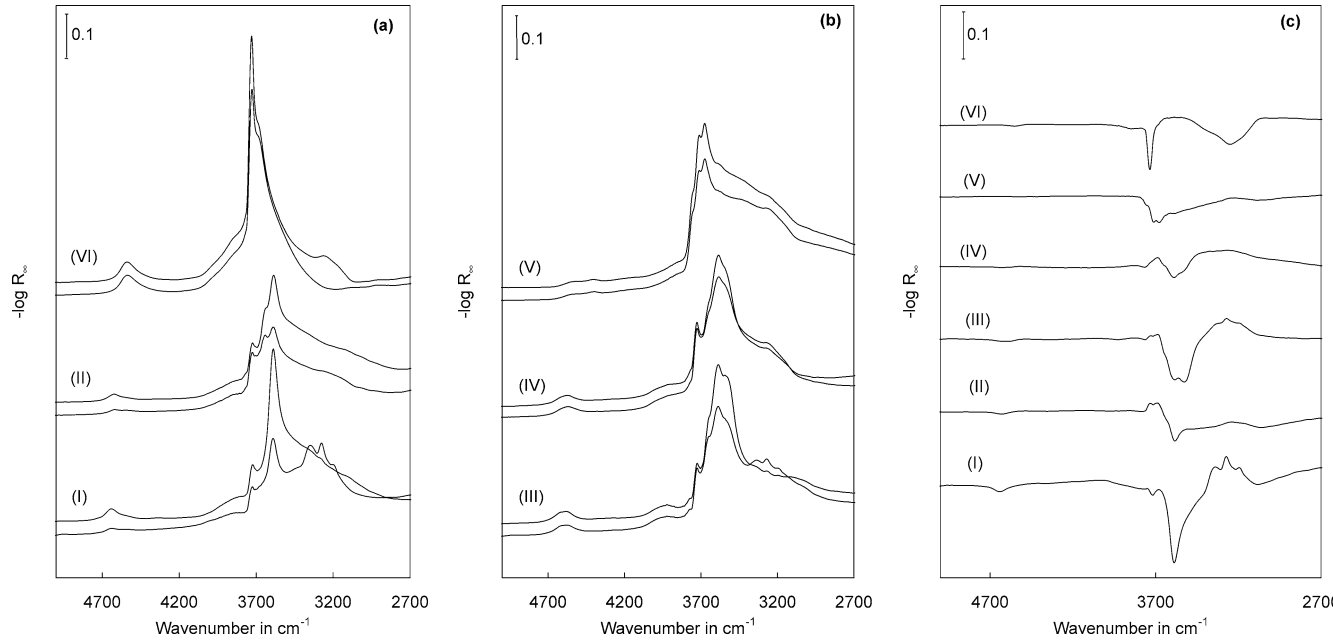

Fig. 3. In situ DRIFT spectra of support (upper lines) and 2 wt% Zn + support (lower lines) recorded at 873 K (a, b); difference spectra (c); Zn+NH_4-ZSM-5 (I), Zn+H-ZSM-5 (II), Zn+NH_4-Y (III), Zn+H-Y (IV), Zn+γ-Al_2O_3 (V), and Zn+SiO_2 (VI).

4620 and 4570 cm^{-1} assigned to combination vibrations of O_1H and O_3H, respectively, were found in the in situ DRIFT spectra of the Y zeolites (Fig. 3b, spectra III and IV). The high-frequency band at 3660, the low-frequency band at 3590, and the band at 3520 cm^{-1} are attributed to O_1H, O_3H, and O_2H-stretching vibrations, respectively [20]. A decrease of the intensity of these bands during the heating process in mixtures with zinc was observed. In contrast to this result, the intensity of the band at 3730 cm^{-1} representing silanol groups remained constant (Figs. 3b and 3c, spectra III and IV).

On the Zn+SiO_2 sample the intensity of the band representing silanol groups (3730 cm^{-1}) decreased upon heating during in situ measurement (Figs. 3a and 3c, spectra VI). Furthermore, the combination vibration band at 4545 cm^{-1} decreased, too. A small shoulder at 3680 cm^{-1} belonging to inaccessible internal or bulk OH groups [21] remained constant.

On γ-alumina different types of stretching vibrations of hydroxyl groups are present (Fig. 3b, spectrum V). The band with the lowest frequency (3675 cm^{-1}) represents a configuration where the OH groups are coordinated to three cations in octahedral interstices. The band with the highest frequency (3760 cm^{-1}) is assigned to terminal OH groups, which are coordinated to either a single octahedral or a single tetrahedral Al^{3+} cation. The band at 3720 cm^{-1} should belong to a bridging OH group, which links either a tetrahedrally with an octahedrally coordinated cation or two octahedrally coordinated cations with each other [21]. All types of bands in the OH-stretching region decreased their intensity if a mixture with zinc was heated (Figs. 3b and 3c, spectra V).

The TPHE treated Zn+NH_4-ZSM-5 and Zn+H-ZSM-5 samples were studied by in situ DRIFT as a function of their zinc content. With increasing zinc content in the mixtures with both types of ZSM-5 zeolites, the band representing the bonding vibration of bridging hydroxyl groups decreased until all of these groups were consumed (Figs. 4a and 4c). The spectra of the mixtures with 5 and 8 wt% Zn+H-ZSM-5 after TPHE treatment have similar characteristics. The silanol band at 3730 cm^{-1} remained constant (Figs. 4a and 4c).

In the skeletal vibration region (Figs. 4b and 4d) bands at 1215–1050 cm^{-1} and 810 cm^{-1} were observed belonging to TO_4 asymmetric and symmetric stretching vibrations, respectively. With increasing zinc content a new band appeared at 920 cm^{-1}, which is assigned to zinc (or other) cations perturbing framework vibrations or zinc ions in complex with ammonia (which would apply for the Zn+NH_4-ZSM-5 zeolite, which is shown later) [22–24]. In the in situ DRIFT spectra of Zn+NH_4-ZSM-5 (Fig. 3a) also bands at 3360, 3275, and 3190 cm^{-1} were observed due to NH-stretching vibrations [24]. These bands were less intense for the TPHE-treated sample with low zinc content (Fig. 4a, spectrum II). With increasing zinc content these bands did not disappear after TPHE treatment (Fig. 4a, spectra III to VI); i.e., the formed species were stable up to 1123 K.

3.3. XANES

A complementary method to throw light on the solid-state redox reaction is the observation of the state of metal species by XANES. Before TPHE treatment, zinc in the mixture with the supports possessed the same XANES spectrum as metallic zinc (Fig. 5, spectra I and II, respectively, and

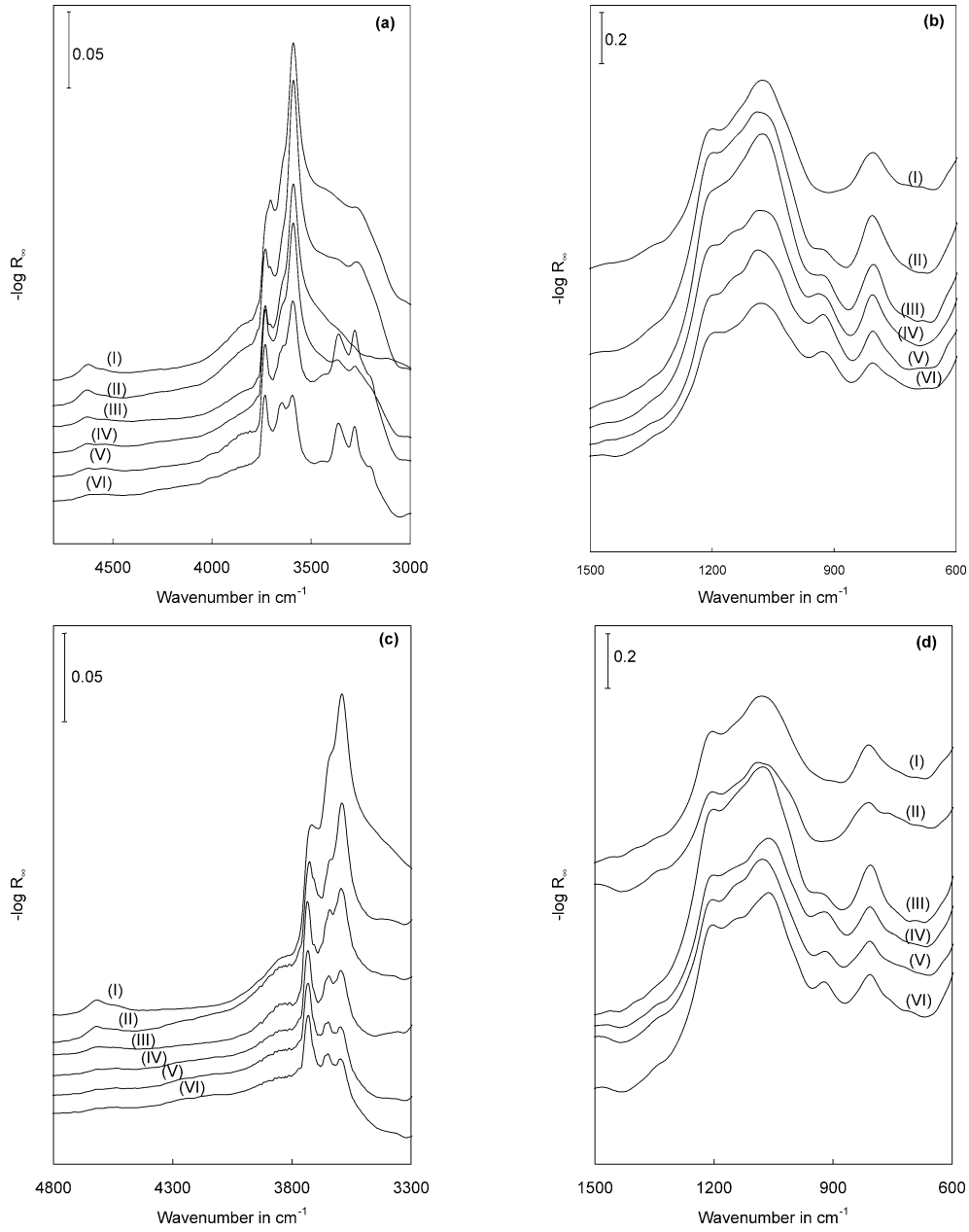

Fig. 4. In situ DRIFT spectra recorded at 873 K on samples after TPHE treatment: Zn+NH_4-ZSM-5 (a, b) and Zn+H-ZSM-5 (c, d); zinc content provided in the support: 0 wt% (I), 1 wt% (II), 2 wt% (III), 3 wt% (IV), 5 wt% (V), 8 wt% (VI).

Table 2). On the other hand, the XANES spectra of zinc ion-exchanged ZSM-5 zeolite and Zn + support mixtures after TPHE treatment were also nearly identical though the intensity of the white line was slightly lower for the latter samples (Fig. 5, spectra III and IV, respectively, and Table 2). There were distinct differences between these spectra of samples containing zinc in the metallic state and those where zinc was supposed to be an ionic species. The Zn *K* edge was shifted to higher values, the intensity of the white line increased, and the edge width decreased for the Zn-ZSM-5 zeolite and the TPHE treated Zn+NH_4-ZSM-5 zeolite (Table 2). In Fig. 5 it can also be seen that the second absorption maximum was shifted remarkably from ∼9.70 to ∼9.72 keV from metallic zinc to zinc ions. The mixtures of zinc with all other supports showed the same characteristics after TPHE treatment as the Zn-ZSM-5 zeolite (Table 2).

3.4. XRD

Fig. 6 shows the XRD results of mixtures of zinc with H-ZSM-5 and H-Y zeolite before and after TPHE treatment. For comparison, also literature data for the pure zeolites are displayed [25]. On the basis of these results, a regular zeolite structure can be concluded for all samples before as well as after TPHE treatment, although the background was higher on the latter samples. On both mixtures before TPHE treat-

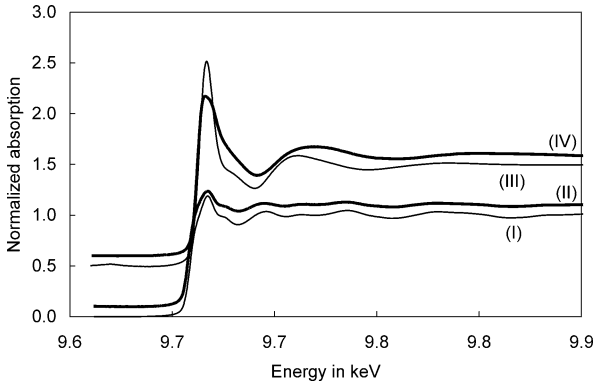

Fig. 5. XANES spectra of Zn (I), Zn+NH_4-ZSM-5 zeolite (II) (bold line), Zn-ZSM-5 prepared by ion exchange in the liquid phase (III), and Zn+NH_4-ZSM-5 after TPHE treatment (IV) (bold line).

Table 2
XANES results obtained on mixtures of zinc with supports (2 wt% Zn)

Sample	Zn *K* edge[a] (eV)	Intensity of white line[b] (a.u.)	Edge width[c] (eV)
Zn^{2+} (4 O) [28][d]		1.58	7.4
Zn^{2+} (5 O) [28][e]		1.80	2.6
Zn^{2+} (6 O) [28][f]		2.12	3.8
Zn	0.0	1.2	8.4
Zn-ZSM-5	4.4	2.0	3.4
Zn-ZSM-5[g]	3.0	1.5	6.0
ZnO	1.9	1.4	7.5
After TPHE treatment			
Zn+NH_4-ZSM-5	3.3	1.6	4.0
Zn+H-ZSM-5	3.3	1.5	3.9
Zn+NH_4-Y	2.3	1.7	4.1
Zn+H-Y	2.7	1.4	3.9
Zn+SiO_2[h]	3.0	1.4	4.9

[a] First inflection point, related to Zn *K* edge of metal foil at 9659 eV.
[b] First absorption maximum.
[c] Difference between first absorption maximum and edge.
[d] Four oxygen ligands in ZnO.
[e] Five oxygen ligands in bis(*N*-benzoylglycinato)triaquazinc(II)-dihydrate.
[f] Six oxygen ligands in bis(hydrogenmaleato)tetraquazinc(II).
[g] Results obtained by in situ dehydration of the sample at 775 K.
[h] 4 wt% zinc.

ment, a reflex for metallic zinc is visible around 43° 2Θ, which disappeared after the treatment (Fig. 6, +).

4. Discussion

In order to discuss the solid-state redox reaction between the different metals and the supports, the samples were thoroughly characterized, both from the viewpoint of acid as well as metal sites. When considering the driving force for the procedure of the reaction, two parameters from the metal side are obvious that could play major roles: melting point to provide sufficient mobility of the metal to approach the acid sites on the solid phase, and the electrochemical potential reflecting how base the metal is. These values are summarized for all investigated metals in Table 3 (taken from [26]).

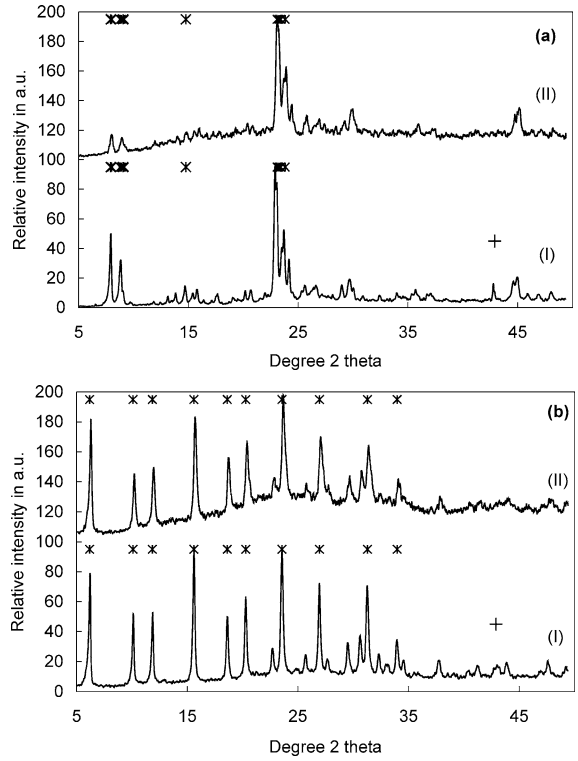

Fig. 6. XRD of Zn+H-ZSM-5 (a) and Zn+H-Y (a) taken before (I) and after (II) TPHE treatment, respectively, reflexes for the pure zeolites according to IZA standards marked with asterisks [25].

Table 3
Melting points and electrochemical potentials of the metals studied in the TPHE experiment sorted by melting points

Metal	Melting point (K)	Electrochemical potential (V)	
Gallium	302.9	$Ga \Leftrightarrow Ga^{3+}$	−0.549
		$Ga \Leftrightarrow Ga^{+}$	−0.200
Tin	505.1	$Sn \Leftrightarrow Sn^{2+}$	−0.138
Zinc	692.7	$Zn \Leftrightarrow Zn^{2+}$	−0.762
Magnesium	923.2	$Mg \Leftrightarrow Mg^{2+}$	−2.372
Aluminum	933.5	$Al \Leftrightarrow Al^{3+}$	−1.662
Manganese	1518.2	$Mn \Leftrightarrow Mn^{2+}$	−1.185
Nickel	1728.3	$Ni \Leftrightarrow Ni^{2+}$	−0.257
Iron	1811.2	$Fe \Leftrightarrow Fe^{2+}$	−0.447
		$Fe \Leftrightarrow Fe^{3+}$	−0.037

The TPHE results gave the first indications for a solid-state redox reaction because the evolved hydrogen is supposed to arise from the reaction. One must, however, be careful to use only this parameter as there could be other sources of hydrogen as well, as will be discussed later. Considering the hydrogen evolution temperatures irrespective of the support, there was a clear correlation with the melting points of the metals (see Fig. 7 and Table 3). There were, however, a few exceptions. The mixtures of zinc with the ammonium forms of ZSM-5 or Y zeolite had significantly lower evolution temperatures compared to all other supports (these values are not included in Fig. 7, see also Table 1). This phenomenon will be discussed later in more

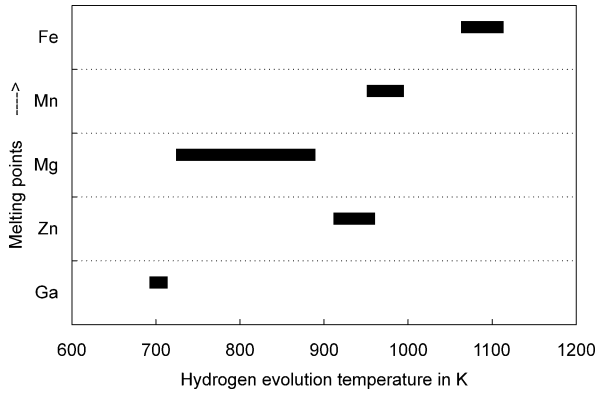

Fig. 7. Temperatures for hydrogen evolution in the TPHE experiment for mixtures of different metals with H-ZSM-5, H-Y zeolites, SiO_2, and γ-Al_2O_3.

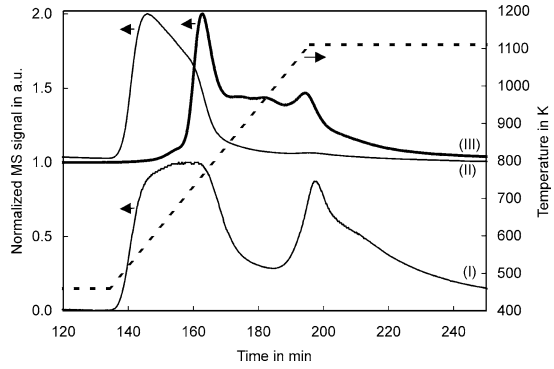

Fig. 8. TPHE spectrum recorded by the ms detector: H_2O signal (mass number 18) on NH_4-ZSM-5 (I) and Mg+NH_4-ZSM-5 (II); H_2 signal (mass number 2) on Mg+NH_4-ZSM-5 (III, bold line); temperature (dotted line, right axis).

detail. Further, magnesium did not fit into the picture because the hydrogen evolution temperatures stretched over an extremely large (and "wrong") temperature range (Fig. 7). Iron when heated with γ-alumina evolved hydrogen at significantly lower temperatures as with the other supports. In this case one might speculate about the formation of spinel-type structures (iron aluminate). Indeed, XRD measurements supported this proposal. The typical reflexes for iron metal at 44.6 and 82.3° 2Θ disappeared nearly after TPHE treatment with γ-alumina and a number of new ones appeared at 30.9, 36.4, 54.9, 58.7, and 64.5° 2Θ thus giving the typical iron-aluminate-spinel pattern.

Finally, some metals were missing, although their melting points lay between those of gallium and iron.

Starting with the last result, the absence of a redox reaction in the case of aluminum and nickel could be explained by a passivation due to the formation of stable oxide layers around the metal particles on air. This layer prevents an efficient melting of the particles and/or attack of the acid sites of the support. A removal by in situ reduction at higher temperatures prior to the experiment would, however, also initiate a solid-state redox reaction itself.

For tin, on the other hand, an additional limiting factor could be the rather high (at least compared to the other metals) electrochemical potential, though the metal is easily dissolved in strong liquid acids. Furthermore, tin is also covered by a thin oxide layer on air.

The behavior of the mixtures of magnesium with the supports was unusual with respect to a number of parameters: (i) the broad temperature range where hydrogen was evolved, which was furthermore too low compared to the other metals (Fig. 7), (ii) the appearance of multiple evolution peaks, and (iii) the inconsistent amounts of evolved hydrogen compared to the other metals (see Table 1). A closer look at the chemical properties of this metal revealed, however, that magnesium is very eager to react with water vapor at higher temperatures to give hydrogen and magnesium oxide. Although there was a drying procedure at 473 K prior to the TPHE treatment, water was not fully desorbed and could thus participate in reactions. The analysis of the effluent gas of the TPHE treatment showed, indeed, that the formation of hydrogen coincided with the desorption of water from the zeolites and the other supports as well (Fig. 8). The water desorption preceded the hydrogen evolution in the TPHE experiment and there was an increase in hydrogen evolution accompanied by the disappearance of water in the effluent stream. This behavior was in contrast to the other samples. Further, there was not observed a high temperature peak of water desorption (dehydroxylation of the supports) on the mixtures with magnesium as on all other samples. Thus, a reaction toward hydrogen without the involvement of the support cannot be excluded at least from these TPHE measurements.

Moreover, DRIFT studies of the mixtures with magnesium did not indicate a decrease of absorption bands related with protonic sites of the supports, which is in line with the assumptions made above.

The XRD analysis of the magnesium-containing H-ZSM-5 zeolite before and after TPHE treatment showed finally (Fig. 9) that the parent material naturally contained the metal magnesium. The corresponding reflexes disappeared completely after TPHE treatment and those for magnesium oxide appeared. Consequently, there was indeed a transition from the metallic state to the oxide. It is thus highly probable that magnesium reacted with the water that was being desorbed from the supports and not with their protons. Therefore, the evolved hydrogen originated from this reaction and not from a solid-state redox reaction.

The discussion above showed that there might occur misinterpretations as to the source of hydrogen when only TPHE studies are considered. It is thus important to include other characterization methods as well. When observing the functional groups of the supports involved in the solid-state redox reaction, namely Brønsted acid sites in the zeolites and silanol groups, in situ DRIFT provided valuable insight in the changes accompanying the heating of the metal + support mixtures. The zinc-containing systems were studied in more detail.

A decrease of absorption bands assigned to bridging hydroxyl groups was observed on both ammonium and

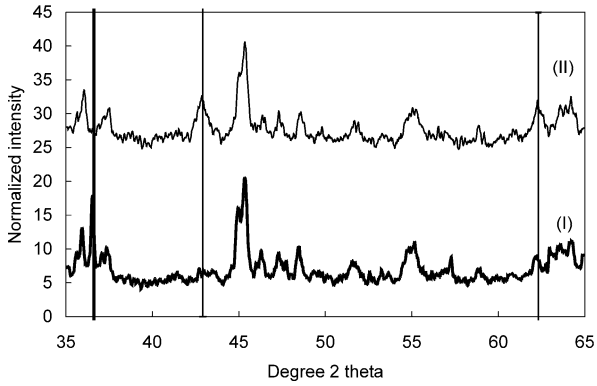

Fig. 9. XRD of Mg+H-ZSM-5 before (I) (bold line) and after TPHE treatment (II) (thin line), vertical lines mark the most intensive reflexes for Mg (bold) and MgO (thin), respectively (other reflexes are due to the zeolite).

protonic forms of Zn+ZSM-5 zeolite mixtures (Figs. 3a and 3c).

On H-ZSM-5 zeolite also bands related to AlOH groups of extraframework species were detected. A decrease of the intensity of these bands in the course of heating Zn+H-ZSM-5 indicated that this type of hydroxyl groups was also involved in the solid-state redox reaction (Figs. 3a and 3c). The effects with respect to changes in the intensity of OH bands were generally less pronounced in the in situ DRIFT compared to the samples measured after TPHE treatment (see Figs. 3 and 4). This was due to the lower final temperatures in the in situ DRIFT cell, which was limited to 873 K (compared to 1123 K in the TPHE treatment).

The intensity of the band representing silanol groups remained constant, which suggests that silanol groups were not involved in the solid-state redox reaction of the ZSM-5 zeolite studied in this work (Figs. 3a and 3c).

If the zinc content were increased until there were a surplus of zinc provided with respect to the amount of Brønsted acid sites in the H-ZSM-5 zeolite (Fig. 4), the spectra had similar features. Conclusively, the solid-state redox reaction took place until all Brønsted acid sites were consumed by reaction with zinc. Even then, no silanol groups of the investigated H-ZSM-5 sample underwent the solid-state redox reaction with the additionally available zinc metal.

In the Y zeolites, the bands in the OH-stretching vibrations region were only slightly resolved already in the parent material (Fig. 3b, spectra III and IV, upper lines). This could be due to extraframework species as an industrial, probably deep-bed-treated, Y zeolite sample was used. However, the changes after TPHE treatment in the bands assigned to hydroxyl groups are nevertheless significant. The same results as in the case of the ZSM-5 zeolite were also obtained for the samples with Y zeolites: the absorption bands of bridging hydroxyl groups at 3660 and 3590 and a small shoulder at 3520 cm^{-1} decreased in all samples during heating. So did the combination vibrations of hydroxyl groups at 4620 and 4570 cm^{-1}. Thus, all types of bridging hydroxyl groups in the Y zeolite underwent the solid-state redox reaction (Figs. 3b and 3c). The silanol groups of the Y zeolites were not involved in the solid-state reaction as already observed on the mixtures with ZSM-5 zeolites (Figs. 3b and 3c).

When evaluating hydroxyl groups by absorption band intensities upon heating, dehydroxylation must be considered, which can lead to overestimations with respect to the extent of solid-state reactions. This disappearance of hydroxyl groups by dehydroxylation did not take place under the conditions applied in the in situ DRIFT measurements. However, under the more severe TPHE treatment conditions, a decrease in the number of Brønsted acid sites caused by dehydroxylation should not be underestimated. However, as the spectra of both the parent support and the mixtures with the metals were always compared after TPHE treatment, the effect of a solid-state redox reaction can be separated from dehydroxylation processes (Fig. 4). A decrease of the crystallinity of the zeolites can be concluded from the XRD measurements before and after treatment on both H-ZSM-5 zeolite and Y zeolites. The increased background in the XRD diffractograms indicates an amorphization of the structure to some extent. However, the zeolitic structure was still pronounced even for the Y zeolite subjected to the TPHE treatment up to 1123 K (Fig. 6).

According to the TPHE experiment, a solid-state redox reaction proceeded on all supports, even SiO_2, the OH groups (silanol) of which are usually regarded as nonacidic (at least compared with zeolites). On the mixture Zn+SiO_2, Brønsted acid sites are absent. In this mixture, the amount of silanol groups decreased by heating (Fig. 3a and 3c). As both spectra were taken at 873 K, a possible dehydroxylation of the silanol groups is already considered and the decrease of the intensity of the band representing silanol groups can be explained in terms of their involvement in the solid-state redox reaction. Not all silanol groups are able to react, but only those accessible by the metal as there remained a small shoulder at 3680 cm^{-1} for inaccessible internal or bulk OH groups [21] (Figs. 3a and 3c).

Finally Zn+γ-Al_2O_3 was investigated by in situ DRIFT. It has a defect spinel structure in which a certain number of cationic positions remain unoccupied. This means that Al^{3+} is tetrahedrally as well as octahedrally coordinated. Hence, different types of stretching vibrations of hydroxyl groups are present. Nevertheless, all types of hydroxyl groups on the γ-alumina surface underwent a solid-state redox reaction as shown by the decrease of all identified bands in the OH-stretching region (3675, 3720, 3760 cm^{-1}, respectively, Figs. 3b and 3c). There should not proceed a phase transition from γ-Al_2O_3 to δ-Al_2O_3 (1023 K [27]) during the in situ DRIFT measurements, which go up to 873 K. However, this cannot be excluded for the TPHE-treated samples (highest temperature 1123 K).

In conclusion, the nature of protonic sites involved in the solid-state redox reaction depended on the support. On zeolites, Brønsted acid sites were involved, whereas on silica silanol groups reacted.

Parallel to the decrease of the bands representing Brønsted acid sites in zeolites a new band appeared at 920 cm^{-1}

after TPHE treatment, which can be assigned to vibration of distorted lattice caused by zinc ions located at extraframework positions. In this way, also the product of the redox reaction, the metal ion, was observed indirectly (Figs. 4b and 4d).

However, the band at 920 cm^{-1} is not specific for ionic zinc species [22–24]. Thus the coordination of the metal itself was further studied using XANES spectroscopy. Usually, preedge peaks due to $1s \rightarrow 3d$ transitions are evaluated in order to determine the coordination geometry of transition metals. There is, however, no preedge peak in case of zinc, because the $3d$ subshell is completely filled. Thus, criteria as the position of the K edge and the intensity of the first absorption maximum together with the difference between these two energy positions (edge width) can be considered when evaluating XANES spectra of zinc samples. By studying zinc-containing complexes having oxygen in the first coordination sphere, the following correlation between the intensity of the white line in the XANES spectrum and the coordination of the metal was reported [28]: octahedrally coordinated zinc > fivefold coordinated zinc > tetrahedrally coordinated zinc. Simultaneously, the edge widths increased (see Table 2). These findings correspond very well to the references studied in this work (see Table 2) and previously [29,30]. When the oxidation number of zinc increased and/or the electronegativity of the ligands, a shift of the Zn K edge toward higher energies was observed [28]. Comparing zinc metal and the TPHE-treated samples, the shift (see Table 1) can accordingly be explained in terms of a substitution of zinc (in metal) by oxygen (in the support) as the first neighbors and an oxidation of the metal as well. The white lines of TPHE-treated samples, on the other hand, had a slightly lower intensity than Zn-ZSM-5 samples prepared by ion exchange though the spectra were otherwise nearly identical (Fig. 5, spectra III and IV). One might expect that these lower values indicate the presence of a mixture of tetrahedrally and octahedrally coordinated zinc species (according to Eggers-Borkenstein [28]) and, thus, an incomplete solid-state redox reaction. However, it was shown previously that a dehydration of Zn-ZSM-5 zeolites prepared by ion exchange by heating them up gave the same result, namely a decrease of the intensity of the white line and a shift of the edge energy to lower values ([30] and Table 1). Consequently, a lower water content is proposed for the Zn + support mixtures after TPHE treatment than the Zn-ZSM-5 samples. When zinc ions are exchanged by conventional methods in solution, the metal ion is surrounded by a hydrate shell when entering the zeolite. These water ligands are present additionally to the water normally adsorbed on the zeolite surface and can be detected in the XANES spectra because of their interaction with the zinc ions. In the course of the solid-state redox reaction, however, zinc metal without a hydrate shell is reacting, yielding zinc ions in the zeolite channels with the same coordination as those in a dehydrated Zn-ZSM-5 zeolite.

Thus, a solid-state redox reaction can be concluded from the XANES results, even on the Zn+SiO_2 mixture giving zinc ions with the same coordination as in Zn-ZSM-5 prepared by conventional ion exchange.

Summarizing these findings, the solid-state redox reaction can take place on various kinds of supports containing protons and low melting (base) metals. The nature of the protonic sites of the supports does not play a major role concerning the temperature where the reaction takes place.

Surprisingly, on mixtures of zinc with the ammonia forms of ZSM-5 and Y zeolites, another picture must be drawn. The hydrogen evolution proceeded at lower temperatures compared to the H-form of the zeolites, silica, and γ-alumina (see Table 1).

When comparing the zeolites with each other, the difference between Zn+NH_4-ZSM-5 and Zn+H-ZSM-5 (or the corresponding Y zeolites) is that on the former sample zinc is present when ammonium ions are converted to protons by release of ammonia. Thus, a driving force must be operational including zinc species and ammonia, which does not work on the other metal samples or other supports. It is known that zinc ions tend to form complexes with ammonia. This could be such a driving force for the reaction to proceed at lower temperatures. The different behavior of protonic and ammonium forms of the ZSM-5 zeolites in contact with zinc can also be seen from the dependence of the maximum of the hydrogen evolution temperature on the amount of supplied zinc. Whereas there is no change on NH_4-ZSM-5, this temperature decreased on H-ZSM-5 (see Fig. 2) with increasing amount of zinc. Thus, the reaction is favored and probably accompanied by other processes in the system Zn+NH_4-ZSM-5 zeolite.

In the in situ DRIFT spectra of the Zn+NH_4-ZSM-5 and Zn+NH_4-Y samples, NH vibrations were identified (Figs. 3a and 3b and Fig. 4a). These bands could be due to ammonia adsorbed on Lewis acid sites, i.e., Zn^{2+} ions formed by solid-state redox reaction, and suggest the formation of zinc–ammonia complexes ($[Zn(NH_x)_y]^{2+}$), which are located in the channels of the zeolite. After the TPHE treatment, these NH bands became rather small. This could be explained by the decomposition of the complex or the desorption of ammonia at elevated temperatures. For higher zinc contents in the mixture with NH_4-ZSM-5 zeolite, these bands were more intense after the TPHE treatment (Fig. 4a). This indicates a rather stable complex with zinc species.

It is further interesting to draw the amount of evolved hydrogen into this discussion. With a higher supply of zinc, 5 wt% Zn in particular, the amount of evolved hydrogen on Zn+NH_4-ZSM-5 suddenly exceeded the theoretical value calculated by assuming a reaction of all zinc submitted in the sample.

Such a phenomenon was not observed on Zn+H-ZSM-5, where the hydrogen evolution remained the same also at zinc provision higher than the amount of protons. In addition, a high-temperature peak started to appear in the TPHE spectrum of Zn+NH_4-ZSM-5. There must thus be a source

for this additional hydrogen. When analyzing the MS signal in the TPHE experiment, the evolution of nitrogen was observed precisely when the amount of evolved hydrogen exceeded the amount of protonic sites. Consequently one must assume a decomposition of ammonia, when in complex with zinc species, which provides surplus hydrogen (and releasing also nitrogen), though the nature of these species is yet not known.

5. Conclusion

The solid-state redox reaction was studied for gallium, tin, zinc, magnesium, manganese, nickel, iron, and aluminum in contact with ZSM-5 and Y zeolites, γ-alumina, and silica. Thus a wide range of properties like melting point and electrochemical potential for the metals and structural and acidic properties for the supports were covered.

It was proven that the solid-state redox reaction proceeded on mixtures of gallium, zinc, manganese, and iron with the supports, including silica-containing silanol groups to a significant extent.

The requirements with respect to the acid properties of the support are rather poor in the way that Brønsted acid sites, extraframework species of the zeolites, and even silanol groups of silica can undergo the solid-state redox reaction depending on which support is used. It is thus also not surprising that hydroxyl groups in γ-alumina take part in the solid-state redox reaction as well.

Considering the metal, a low melting point combined with a very negative electrochemical potential are necessary requirements for the reaction to proceed. The low electrochemical potential governs the reaction itself. The low melting point, on the other hand, provides sufficiently mobile metal species to reach the acid sites and thus determines the temperature at which the solid-state redox reaction proceeds.

An interesting result for zinc in combination with ammonia forms of zeolites was that there is obviously a complex formation with ammonia facilitating the solid-state redox reaction. Further, a decomposition of ammonia took place giving additional hydrogen (and nitrogen). The nature of zinc species responsible for this decomposition is not yet known.

The hydrogen evolution observed on samples containing magnesium can easily be misinterpreted as a solid-state redox reaction. It originated, however, from the reaction of the metal with water adsorbed on the supports.

Generally, the solid-state redox reaction was shown to be very useful for obtaining supported acid catalysts with high exchange degrees, saving time, chemicals, and waste to be disposed.

Acknowledgments

The authors are grateful for financial support provided by the Deutsche Forschungsgemeinschaft in the frame of the Priority Program: From ideal to real systems: Bridging the pressure and materials gap in heterogeneous catalysis. Thanks go to HASYLAB for providing beamtime at E4. The authors are thankful to K. Klementiev for valuable experimental assistance in the XANES experiments, E. Loeffler (Ruhr University Bochum, Germany) for helpful discussions about DRIFT, and A. Schoeneberg and L.L. Berring (Technical University of Denmark, Lyngby, Denmark) for XRD measurements.

References

[1] A. Hagen, F. Roessner, Catal. Rev. Sci. Eng. 42 (2000) 403.
[2] U. Mroczeck, W. Reschetilowski, K. Pietzsch, K.H. Steinberg, React. Kinet. Katal. Lett. 43 (1991) 539.
[3] N.W. Cant, I.O.Y. Liu, Catal. Today 63 (2000) 133.
[4] R.Q. Long, R.T. Yang, J. Catal. 207 (2002) 274.
[5] L.V. Pirutko, V.S. Chernyavsky, A.K. Uriarte, G.I. Panov, Appl. Catal. A 227 (2002) 143.
[6] B. Nkosi, F.T.T. Ng, G.L. Rempel, Appl. Catal. A 161 (1997) 153.
[7] J.L. Sotelo, M.A. Uguina, J.L. Valverde, D.P. Serrano, Ind. Eng. Chem. Res. 32 (1993) 2548.
[8] H.K. Beyer, H.G. Karge, G. Borbély, Zeolites 8 (1988) 79.
[9] H.G. Karge, H.K. Beyer, G. Borbély, Catal. Today 3 (1988) 41.
[10] H.G. Karge, G. Borbély, H.K. Beyer, G. Onyestyak, in: M. Philips, M. Ternan (Eds.), Proc. Int. Congr. Catal., 9th, vol. 1, Chem. Inst. Canada, Ottawa, 1988, p. 396.
[11] G. Borbély, H.K. Beyer, L. Radics, P. Sandor, H.G. Karge, Zeolites 9 (1989) 428.
[12] Y.-G. Li, W.-H. Xie, S. Yong, Appl. Catal. A 150 (1997) 231.
[13] M. Rauscher, K. Kesore, R. Mönning, W. Schwieger, A. Tißler, T. Turek, Appl. Catal. A 184 (1999) 249.
[14] A. Hagen, F. Roessner, Stud. Surf. Sci. Catal. 83 (1994) 313.
[15] P.B. Peapples-Montgomery, K. Seff, J. Phys. Chem. 96 (1992) 5962.
[16] A. Seidel, B. Boddenberg, Chem. Phys. Lett. 249 (1996) 117.
[17] H.K. Beyer, G. Pal-Borbely, M. Keindl, Micropor. Mesopor. Mater. 31 (1999) 333.
[18] J. Heemsoth, E. Tegeler, F. Roessner, A. Hagen, Micropor. Mesopor. Mater. 46 (2001) 185.
[19] A. Seidel, G. Kampf, A. Schmidt, B. Boddenberg, Catal. Lett. 51 (1998) 213.
[20] H.G. Karge, M. Hunger, H.K. Beyer, in: J. Weitkamp, L. Puppe (Eds.), Catalysis and Zeolites—Fundamentals and Applications, Springer, Berlin, 1999, p. 211.
[21] G. Mestl, H. Knözinger, in: G. Ertl, H. Knözinger, J. Weitkamp (Eds.), Handbook of Heterogeneous Catalysis, vol. 2, VCH, Weinheim, 1997, p. 563.
[22] G.D. Lei, B.J. Adelman, J. Sárkány, W.M.H. Sachtler, Appl. Catal. B 5 (1995) 245.
[23] H.-Y. Chen, X. Wang, W.M.H. Sachtler, Phys. Chem. Chem. Phys. 2 (2000) 3083.
[24] Z. Sobalík, Z. Tvuraůžková, B. Wichterlová, J. Phys. Chem. B 102 (1998) 1077.
[25] IZA structure commission, Database of zeolite structures at: http://www.iza-structure.org/databases/.
[26] D.R. Lide (Ed.), CRC Handbook of Chemistry and Physics, 76th ed., CRC Press, Boca Raton, FL, 1995–1996, pp. 8–21.
[27] A.F. Hollemann, E. Wiberg, N. Wiberg, in: A.F. Hollemann, E. Wiberg (Eds.), Lehrbuch der Anorganischen Chemie, vol. 101, Walter de Gruyter, Berlin, 1995, p. 1082.
[28] P. Eggers-Borkenstein, Ph.D. thesis, Westfälische Wilhelms Universität Münster, 1989.
[29] C. Henning, F. Thiel, K.-H. Hallmeier, R. Szargan, A. Hagen, F. Roessner, Spectrochim. Acta A 49 (1993) 1495.
[30] A. Hagen, K.-H. Hallmeier, C. Henning, R. Szargan, T. Inui, F. Roessner, Stud. Surf. Sci. Catal. 94 (1995) 195.